Fermi Surface and Extended van Hove Singularity in the Noncuprate Superconductor Sr_2RuO_4

D. H. Lu, M. Schmidt, T. R. Cummins, and S. Schuppler
Forschungszentrum Karlsruhe, INFP, P.O. Box 3640, D-76021 Karlsruhe, Germany

F. Lichtenberg* and J. G. Bednorz
IBM Research Division, Zürich Research Laboratory, CH-8803 Rüschlikon, Switzerland
(Received 22 December 1995)

We mapped the Fermi surface of the first copper-free layered perovskite superconductor, Sr_2RuO_4, by high-resolution ($\approx$22 meV) angle-resolved photoemission. Three bands cross the Fermi energy, consistent with band structure calculations; one around $\overline{\Gamma}$ and two around $\overline{X}$. The highlight is the observation of an extended van Hove singularity located 17 meV below the Fermi level. It extends around $\overline{M}$ for ≈ 0.2 Å^{-1} along $\overline{\Gamma}$-$\overline{M}$-$\overline{\Gamma}$ and $\overline{X}$-$\overline{M}$-$\overline{X}$ in the projected Brillouin zone. This raises important questions related to the possible role of a van Hove singularity for oxide superconductivity. [S0031-9007(96)00410-3]

PACS numbers: 79.60.Bm, 73.20.Dx, 74.70.Ad, 74.80.Dm

Following the discovery of superconductivity in $La_{2-x}Ba_xCuO_4$ by Bednorz and Müller [1], a large number of related compounds with high superconducting transition temperatures (T_c's) has been found. The most common feature of these high-temperature superconductors (HTSC's) is a layered-perovskite crystal structure containing a planar CuO_2 network. It is now generally believed that the conduction takes place in the CuO_2 planes which, therefore, are essential to HTSC's. This raises the question of whether superconductivity can occur in layered perovskites that do not contain copper and why copper is so conducive to high T_c's.

With this key question in mind, the recent discovery of superconductivity in Sr_2RuO_4 ($T_c = 0.93$ K) by Maeno *et al.* [2] is very significant: This is the first copper-free superconductor to be isostructural to any cuprate superconductor. To understand the nature of the oxide superconductors a thorough understanding of the electronic structure is a prerequisite. Some readily apparent difference of Sr_2RuO_4 to HTSC's include the following: (1) It is superconducting without any chemical doping, whereas superconductivity in the cuprates appears only after carrier doping of an insulating parent compound such as La_2CuO_4; (2) Ru^{4+} ($4d^4$) is in the low-spin state with spin 1, whereas the Cu^{2+} ($3d^9$) valence state has spin 1/2; and (3) the d orbitals involved in the d-p hybridization have t_{2g} (d_{xy}, d_{xz}, and d_{yz}) in Sr_2RuO_4 but e_g ($d_{x^2-y^2}$) symmetry in the copper oxides.

As amply demonstrated for the HTSC's [3], angle-resolved photoemission spectroscopy (ARPES) is a powerful method of measuring the electronic structure close to the Fermi level (E_F). In this Letter, we present ARPES data from single-crystalline Sr_2RuO_4 (Ref. [4]). With high energy resolution we have mapped the whole Fermi surface (FS) in the reduced Brillouin zone (BZ). The measured FS is compared with local-density-approximation (LDA) band structure calculations [5,6].

The Sr_2RuO_4 single crystals were grown in air by a modified floating-zone melting process [7]. The crystals can easily be cleaved, yielding highly oriented crystals with a (001) surface. Electrical resistivity measurements performed on crystals from the same batch give a T_c of 0.93 ± 0.03 K [2]. The crystal structure is body-centered tetragonal of the K_2NiF_4 type with $a = b = 3.8694$ Å and $c = 12.746$ Å at room temperature as determined by x-ray powder diffraction [8].

ARPES measurements were performed with a discharge lamp using the Ne I line at 16.85 eV (the satellite line at 16.67 eV has no intensity contribution in the narrow energy range of the spectra of this work). The angular acceptance of the hemispherical analyzer (VSW HA50) was $\pm 1°$, which corresponds to a $\mathbf{k}$ resolution of 0.06 Å^{-1}. A pass energy of 2 eV was chosen, corresponding to an energy resolution of 22 meV as determined by the Fermi edge of freshly evaporated gold films at 10 K. The single crystals were oriented with Laue diffraction; then, once inside the analysis chamber, the relative sample orientation could be determined to within $\pm 1°$ using a charge-coupled device camera. The samples were cooled down to 10 K and then cleaved *in situ* at a pressure of $< 3 \times 10^{-11}$ mbar. Even at such a low pressure, the sample surface becomes contaminated, and reliable spectra can only be recorded up to 12 h after cleaving. During the measurements, we checked the spectra regularly to ensure that no changes has occurred. After completion of the measurements, the sample orientation was confirmed by low-energy electron diffraction.

Figure 1 presents ARPES data for Sr_2RuO_4 along three high-symmetry lines. The high two-dimensional character allows us to adopt the projected BZ. Since we are interested in measuring the Fermi surface, we concentrate only on a very narrow energy range near E_F. A study on the full valence band will appear elsewhere [9]. The angles (θ, ϕ) displayed next to each energy distribution curve

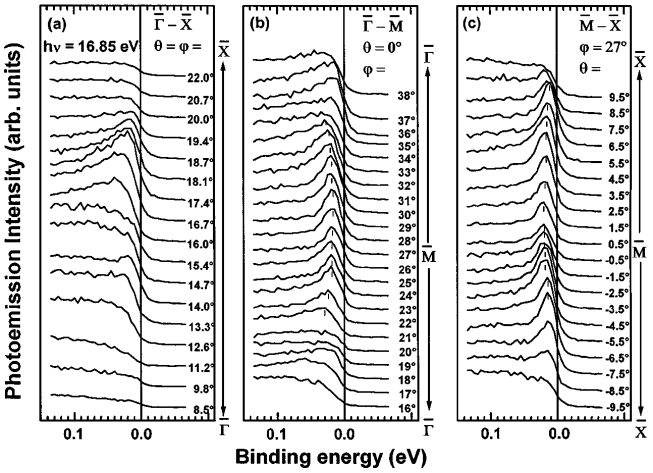

FIG. 1. Experimental ARPES spectra from Sr_2RuO_4 using $h\nu = 16.85$ eV photons along the (a) $\overline{\Gamma}$-$\overline{X}$, (b) $\overline{\Gamma}$-$\overline{M}$-$\overline{\Gamma}$, and (c) $\overline{X}$-$\overline{M}$-$\overline{X}$ directions.

(EDC) in Fig. 1 denote the emission direction of the collected photoelectrons (with kinetic energy E_k). They are related to $\mathbf{k}_{\|} = (k_x, k_y)$ via $k_x = (\sqrt{2mE_k}/\hbar)\sin\theta$, $k_y = (\sqrt{2mE_k}/\hbar)\sin\phi$. Figure 1(a) shows the EDC's along the $\overline{\Gamma}$-$\overline{X}$ direction. Starting from the lowest spectrum in the series and moving up to larger angles, a peak is seen to emerge from the background at $(\theta, \phi) = 12.6°,12.6°$ and disperses towards E_F. By $(\theta, \phi) = 14.0°,14.0°$, the Fermi level is slightly above the middle of the leading edge of the feature, and by $(\theta, \phi) = 14.7°,14.7°$, the peak has lost the majority of its intensity, indicating a FS crossing between 14.0°,14.0° and 14.7°,14.7°. Starting at $(\theta, \phi) = 16.0°,16.0°$, we see a more pronounced feature disperse towards E_F. Then this feature exhibits more complicated behavior: At $(\theta, \phi) = 18.1°,18.1°$, it has lost part of its intensity, but can still be clearly seen to disperse further towards E_F. It is not before an angle between 18.7°,18.7° and 19.4°,19.4° that a clear FS crossing finally occurs. Figure 1(b) depicts the EDC's along the $\overline{\Gamma}$-$\overline{M}$-$\overline{\Gamma}$ direction. A weakly defined feature is seen to cross E_F at $(\theta, \phi) = 0°,19°$. A more pronounced feature crosses E_F at $(\theta, \phi) = 0°,35°$, which is equivalent to the 0°,19° crossing, reflecting the symmetry about $\overline{M}$. As shown by the tick marks in Fig. 1(b), a second peak emerges from the background at approximately $(\theta, \phi) = 0°,21°$ and disperses towards E_F until $(\theta, \phi) = 0°,23°$. For angles between 0°,23° and 0°,30°, this strong, sharp peak remains in close proximity to E_F, without any evidence for a FS crossing. It then disperses back from E_F when moving away from the $\overline{M}$ point. Figure 1(c) presents the EDC's along the $\overline{X}$-$\overline{M}$-$\overline{X}$ direction, which is perpendicular to the $\overline{\Gamma}$-$\overline{M}$-$\overline{\Gamma}$ direction. The same peak (highlighted by tick marks) again shows no significant changes in energy position from $\theta = -4.5°$ to $\theta = 4.5°$. However, it disperses up towards E_F as we probe further away from the $\overline{M}$ point. Symmetry-equivalent FS crossings are evident at $\theta = \pm 8.5°$.

Figure 2 summarizes the dispersion of this band around the $\overline{M}$ point along both the $\overline{\Gamma}$-$\overline{M}$-$\overline{\Gamma}$ and $\overline{X}$-$\overline{M}$-$\overline{X}$ directions. The peak positions were obtained by fitting a simple spectral function to the EDC's: A product of a Fermi function and a Lorentzian modeling the lifetime-broadened intrinsic line shape of the quasiparticle state was adopted and then convoluted with a Gaussian to represent the analyzer function. A Shirley-type background was included to account for secondary electron losses. The fitting was found to agree quite well with the experimental spectra. The dispersion of this band characterizes a saddle point in the E vs $\mathbf{k}$ space, i.e., a minimum in one direction and a maximum along the perpendicular direction. Such a saddle point is called a van Hove singularity (VHs) [10]. The saddle point we observe here is located at $E_{\mathrm{VHs}} = 17$ meV below E_F and extends in $\mathbf{k}$ space about 0.2 Å^{-1} along both $\overline{\Gamma}$-$\overline{M}$-$\overline{\Gamma}$ and $\overline{X}$-$\overline{M}$-$\overline{X}$ in the projected BZ. This is the first time that such a saddle point singularity has been observed to extend in both directions. In a two-dimensional system, a simple saddle point gives a logarithmic divergence in the density of states (DOS) [10]. A saddle point with an extension in

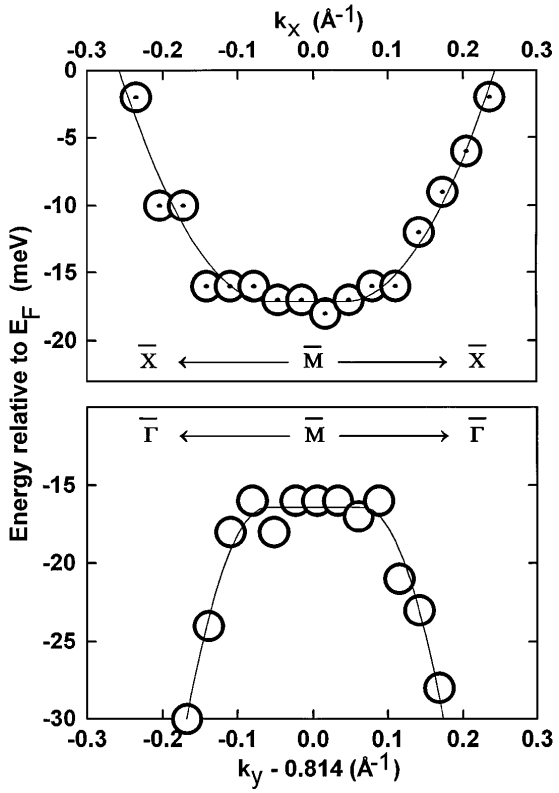

FIG. 2. van Hove singularity around the $\overline{M}$ point in the projected BZ: dispersion along (a) $\overline{X}$-$\overline{M}$-$\overline{X}$ and (b) $\overline{\Gamma}$-$\overline{M}$-$\overline{\Gamma}$. Circles denote the peak positions obtained by a fitting procedure (see text); the solid line is a guide to the eye. The $\overline{M}$ point is represented by $k_x = 0$ and $k_y = 0.814$ Å^{-1}.

only one direction yields a stronger divergence in the DOS such as $(E - E_{\mathrm{VHs}})^{-1/2}$ or $(E_{\mathrm{VHs}} - E)^{-1/2}$. In our case, however, the saddle point extends in both directions, producing a divergence in the DOS such as $|E - E_{\mathrm{VHs}}|^{-1/2}$.

A Fermi surface of Sr_2RuO_4 using the full set of our APRES data throughout the BZ is presented in Fig. 3. The open circles denote the measured positions where the bands cross E_F in the projected BZ, and the solid lines represent the results of a state-of-the-art LDA band structure calculation of Singh [5]. In this calculation, a VHs was predicted to be 60 meV above E_F. In order to compare the calculation with our results, we have shifted the calculated Fermi energy up by 77 meV, thus aligning the calculated VHs position with that obtained experimentally. We observed three bands to cross E_F. This is consistent with the band structure calculations [5,6] which also assign predominantly Ru $4d_{xz,yz,xy}$ character to these bands. The two holelike surfaces centered at $\overline{X}$ agree rather well with the calculation [5], while the electronlike surface around the $\overline{\Gamma}$ point, although finding less agreement, still exhibits a similar topology. We can see from the FS mapping that along $\overline{\Gamma}$-$\overline{X}$ two crossings are very close to each other, thus explaining the complex crossing behavior observed and discussed in Fig. 1(a). A shift of the calculated Fermi energy as employed in the comparison above could, in principle, be caused by deviations from stoichiometry leading to electron doping, as shown in Ref. [5]. However, by quantitative evaluation of the areas enclosed by the Fermi surface, we find that the two hole pockets are filled by 1.5 and 1.8 electrons, while the electronlike band contains 0.7 electron. These values add up to the expected value, 4, for stoichiometric Sr_2RuO_4, thus suggesting that the band structure calculation does not describe the position of the Fermi energy correctly. Previous ARPES experiments on HTSC's have demonstrated a saddle point singularity at $\mathbf{k}_{\parallel} = (\pi/a, 0)$ for $YBa_2Cu_3O_{7-\delta}$ (Y123) [11], $YBa_2Cu_4O_8$ (Y124) [11,12], $Bi_2(Sr_{0.97}Pr_{0.03})_2CuO_{6+\delta}$ (Bi2201) [13], $Bi_2Sr_2CaCu_2O_{8+\delta}$ (Bi2212) [14], and $Nd_{1.85}Ce_{0.15}CuO_4$ (NCCO) [15]. Table I compares the T_c, the temperature dependence of the in-plane normal-state resistivity, $\rho_{ab}(T)$, and the energy position of the VHs relative to E_F of these five cuprates and Sr_2RuO_4. All compounds except NCCO have a VHs very close to E_F and show a linear $\rho_{ab}(T)$. However, NCCO exhibits a T^2 temperature dependence [16] and has a VHs far below E_F.

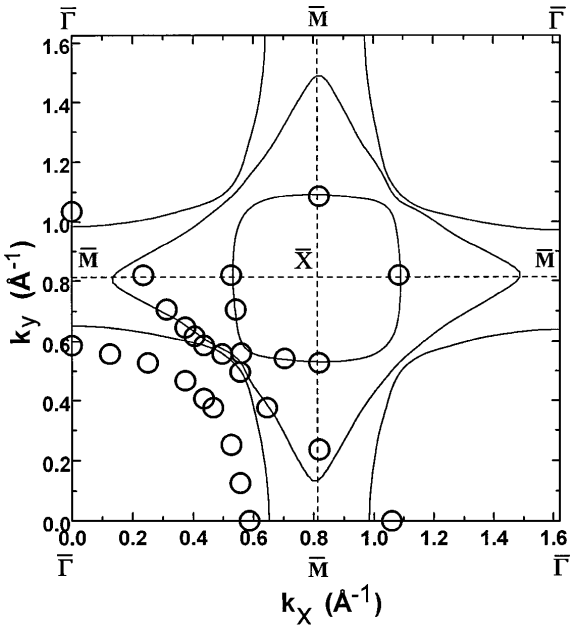

FIG. 3. Measured Fermi surface of Sr_2RuO_4. Open circles denote the FS crossings deduced from ARPES, with a size representative of the resolution. The solid lines denote the Fermi surface derived from the band structure calculation of Singh [5] in the following way: The calculated E_F was shifted by 77 meV to place the theoretical VHs at the experimental value (see text), and the resulting FS is displayed superimposed on the projected BZ.

Taking the evidence from Table I into consideration, there seems to be a common relationship between a VHs close to E_F and a linear temperature dependence of the normal-state resistivity. This has been addressed theoretically in the work of Lee and Read [17]. However, a direct link of a VHs near E_F to a high T_c cannot be made. Invoking standard BCS theory in conjunction with the diverging DOS, several models generically classed as the van Hove scenario have been postulated, which attempt to link the presence of a VHs close to E_F to high T_c's [18]. Such an argument, however, seems to be at odds with the low T_C observed for Bi2201 and Sr_2RuO_4. We can speculate that a high T_c depends strongly on the extent of the VHs, consistent with the fact that the extent of the saddle point is smaller for Bi2201 than found in Y123, Y124, and Bi2212. In the present case, for Sr_2RuO_4, the fact that the VHs extends in both directions might have further consequences which still remain unclear at this time. Of course, we cannot rule out that T_c in Bi2201 and Sr_2RuO_4 is suppressed by other effects. For Sr_2RuO_4 with its close proximity to a ferromagnetic phase [19], ferromagnetic spin fluctuations

TABLE I. The superconducting transition temperature, the temperature dependence of the in-plane normal-state resistivity, and the position of the VHs relative to E_F for cuprate superconductors and Sr_2RuO_4.

	T_c (K)	$\rho_{ab}(T)$	E_{VHs} (meV)
$YBa_2Cu_3O_{7-\delta}$	92	linear	<10[a]
$YBa_2Cu_4O_8$	82	linear	19[b]
$Bi_2(Sr_{0.97}Pr_{0.03})_2CuO_6$	10	linear	<30[c]
$Bi_2Sr_2CaCu_2O_{8+\delta}$	83	linear	<30[d]
$Nd_{1.85}Ce_{0.15}CuO_4$	25	quadratic	350[e]
Sr_2RuO_4	0.93	$\approx$ linear[f]	17[g]

[a]Ref. [11], [b]Ref. [11,12], [c]Ref. [13], [d]Ref. [14], [e]Ref. [15], [f]Ref. [20], and [g]this work.

could conceivably depress T_c. In any case, the low T_c's observed in Bi2201 and also in Sr_2RuO_4 imply that a simple connection between the presence of a VHs close to E_F and a high T_c does not exist.

In summary, we have mapped the FS of Sr_2RuO_4 and found three bands to cross E_F. The topology of the FS qualitatively agrees with LDA band structure calculations. Intriguingly, a saddle point extended in two perpendicular directions was observed 17 meV below E_F at the $\overline{M}$ point in the projected BZ. This finding in a noncuprate layered-perovskite superconductor should provoke further investigations into the possible connection between a van Hove singularity and superconductivity.

We are grateful to Dr. D. Singh for fruitful discussions and for making available the full data set of his band structure calculations. D.H.L. thanks the VW Foundation and the DAAD for financial support.

*Present address: Varta Batterie AG, D-65779 Kelkheim, Germany.

[1] J. G. Bednorz and K. A. Müller, Z. Phys. B **64**, 189 (1986).
[2] Y. Maeno *et al.*, Nature (London) **372**, 532 (1994).
[3] Z.-X. Shen *et al.*, Science **267**, 343 (1995).
[4] After submission of our paper, we became aware of the work by T. Yokoya *et al.* [Phys. Rev. Lett. **76**, 3009 (1996)] on the same subject. An earlier account on some parts of that work was published in T. Yokoya *et al.*, J. Phys. Chem. Solids **56**, 1885 (1995).
[5] D. J. Singh, Phys. Rev. B **52**, 1358 (1995).
[6] T. Oguchi, Phys. Rev. B **51**, 1385 (1995).
[7] F. Lichtenberg *et al.*, Appl. Phys. Lett. **60**, 1138 (1992).
[8] L. Walz and F. Lichtenberg, Acta Crystallogr. Sect. C **49**, 1268 (1993).
[9] M. Schmidt *et al.*, Phys. Rev. B (to be published).
[10] L. van Hove, Phys. Rev. **89**, 1189 (1953).
[11] K. Gofron *et al.*, J. Phys. Chem. Solids **54**, 1193 (1993).
[12] K. Gofron *et al.*, Phys. Rev. Lett. **73**, 3302 (1994).
[13] D. M. King *et al.*, Phys. Rev. Lett. **73**, 3298 (1994).
[14] D. S. Dessau *et al.*, Phys. Rev. Lett. **71**, 2781 (1993); J. Ma *et al.*, Phys. Rev. B **51**, 3832 (1995).
[15] D. M. King *et al.*, Phys. Rev. Lett. **70**, 3159 (1993).
[16] C. C. Tsuei *et al.*, Physica (Amsterdam) **161C**, 415 (1989); Y. Hidaka and M. Suzuki, Nature (London) **338**, 635 (1989); S. J. Hagen *et al.*, Phys. Rev. B **43**, 13 606 (1991).
[17] P. A. Lee and N. Read, Phys. Rev. Lett. **58**, 2691 (1987).
[18] J. E. Hirsch and D. J. Scalapino, Phys. Rev. Lett. **56**, 2732 (1986); R. S. Markiewicz, J. Phys. Condens. Matter **2**, 665 (1990); C. C. Tsuei *et al.*, Phys. Rev. Lett. **65**, 2724 (1990); P. C. Pattnaik *et al.*, Phys. Rev. B **45**, 5714 (1992); D. M. Newns *et al.*, Phys. Rev. Lett. **69**, 1264 (1992); C. C. Tsuei *et al.*, Phys. Rev. Lett. **69**, 2134 (1992); A. A. Abrikosov *et al.*, Physica (Amsterdam) **256C**, 73 (1993); D. M. Newns *et al.*, Phys. Rev. B **52**, 13 611 (1995).
[19] R. J. Cava *et al.*, Phys. Rev. B **49**, 11 890 (1994); S. A. Carter *et al.*, Phys. Rev. B **51**, 17 184 (1995).
[20] Recently, A. P. Mackenzie *et al.* [Phys. Rev. Lett. **76**, 3786 (1996)] showed that $\rho_{ab}(T)$ can be regarded as approximately linear only for $T > 25$ K, in apparent contrast to Ref. [2].